Nature Environment and Pollution Technology
An International Quarterly Scientific Journal

p-ISSN: 0972-6268
e-ISSN: 2395-3454

Vol. 17 | No. 2 | pp. 349-358 | 2018

Original Research Paper | Open Access

Study on Sand-blocking Benefits of Aeolian - Retaining Structures Along the Railway

Wang Lian, Jian-jun Cheng†, Ling-yan Zhi and Lin-gui Xin
College of Water Resources and Architectural Engineering, Shihezi University, Shihezi, China
†Corresponding author: Jian-jun Cheng

Nat. Env. & Poll. Tech.
Website: www.neptjournal.com

Received: 09-08-2017
Accepted: 24-10-2017

Key Words:
Aeolian disaster
Wind tunnel test
Numerical simulation
PE net
Wind profile

ABSTRACT

In view of the frequent occurrence of wind sand disaster in the Gobi area, engineering protection measures aimed at sand-blocking and sand-controlling along the railway are urgently needed to be constantly improved. This paper has analysed the sand-blocking benefits of three aeolian-retaining structures in actual projects through the way of theoretical analysis, wind tunnel test and numerical simulation. The results are as follows: Three engineering measures can reduce the turbulence of the flow and weaken the velocity so that the sand can be deposited easily; under the influence of the solid wall and hanging-style plate sand-retaining wall with 30% porosity, the airflow will form a wide range of vortex zone behind the barrier and there will be an increasing velocity area on the top of the aeolian-retaining wall because of the effect of extrusion. So, these two structures can only be used in smaller wind velocity areas (V<12m/s), and it is also needed to take the effects of negative pressure behind the barriers into account. PE net with 55% porosity can form a more stable flow field behind the net and weaken the airflow at the same time, which is conducive to the control of the movement of sand and can avoid the erosion hazards on the ground caused by the eddy current, and the control effect of PE net on the velocity can be increased up to 15H behind the net. Considering the cost, service life and other conditions of the sand-retaining structures in the wild environment, the PE net would occupy an important position in the sand-controlling along the railway.

INTRODUCTION

The northwest of China belongs to arid area, and there have been occurrence of sandstorm disasters every year, especially in the Gobi and desert areas. The gravel carried by the gale has caused a strong destruction to the vegetation on the surface, structures and the vehicles running on lines. The sandstorms continue to occur along the railway under the influence of the cold wind mainly because of the large quantity of sand existing along the railway (Sun et al. 2004, Gao et al. 2004, Yang et al. 2008, Ren et al. 2006). When the sand exceeds the top of the track about 3cm, it may cause locomotives or vehicles derailment, also will lead to train outage, blow and personnel injuries under special condition, so there is an urgent need to layout sand-proof structures along the railway which locates in the Gobi. Nowadays, engineering measures about sand-proof structures in the blown sand area are universal, including sand-blocking, sand fixation, sand-grooming and sediment transport. High-parallel sand-barrier plays the role of sand blocking mainly, and sets 1 to 3 rows according to the amount of sediment transport. Generally, it includes the entity sand-retaining wall, the void retaining wall and nylon network sand barrier and stands on the outer edge of the protective zone distance to the base of slope of roadbed from 100m to 300m (He 2013). The void sand-retaining wall includes the sleeper-type retaining wall, the hanging plate and the oblique insert plate retaining wall with a porosity of 30% and the nylon barrier network with a porosity of 55% generally. Lot of scholars have done research and analysis on the benefits of the various types of sand-retaining structures in the actual project. It can reduce the cost of the budget and labour's flow and waste for it layout the barriers no longer by the engineering experience alone or the regular observation results in the field, which being interfered with a variety of factors. However, the governance work about the blown sand hazard in our country has been officially launched since the 1990s (Hu 2003), the study on the mechanism of sand movement and the effectiveness of the sand-retaining structure is still in the preliminary exploration stage. Most scholars did detailed analysis only for a single problem usually and lack the multivariate control contrast process of the experimental study. Such as, Li & Jiang (2016) two-dimensional numerical simulation analysis of the wind-retaining wall existed along the Lanzhou Xinjiang railway. Study of Cheng et al. (2016a, b) on the effectiveness of the void wall existed (including hanging-style plate and slant insert plate sand-retaining wall) along the railway. Kang et al. (2015) made observation and analysis in the field of the nylon net on the effect of sand-blocking and sand fixation in the desert area.

Table 1: The relationship between sand particle size and starting wind velocity.

Diameter (mm)	0.1~0.25	0.25~0.50	0.50~1.00	>1.00
Starting velocity (m/s)	4.0	5.6	6.7	7.1

Note: The starting velocity in the table is the velocity value in two metres above the ground.

The governance work on blown sand is continuing and seeking practical and effective measures to prevent blown sand in becoming the focus of attention. Taking the multivariate of field observation experiments and the maturity of computer technology into account, based on the understanding of computational fluid dynamics related software, in this paper, the three-dimensional numerical simulation method is used to compare the surrounding flow field changes of the solid sand-retaining wall. The hanging style sand-retaining wall with 30% porosity and 55% porosity of the PE network, is as shown in Fig. 1. This paper analysed the influence of the three kinds of wind-resisting structures to the blown sand movement to determine the reasonable engineering sand-proof measures.

Fig. 1: Aeolian hazard along the railway (A) and three aeolian-retaining structures (B, C, D).

THEORETICAL FOUNDATION

Wind and sand movement mechanism: The blown sand movement includes the start, migration and deposition process, which is called the erosion and accumulation to the ground, and occurs in the near surface layer usually, mainly concentrating in the air layer near ground from 0 to 2m. The start of the sand is related to the wind velocity and the wind that has caused the blown sand movement is always characterized by turbulence. The results of desertification in China show that the relationship between sand threshold velocity and particle size can be found as provided in Table 1 (Ding 2010).

When the wind velocity exceeds the starting wind velocity, the sand on the surface begins to move, according to the main momentum sources of the sand movement and the difference of wind power, particle size and quality. Bagnold (1941) divided the sand movement into three basic forms i.e., creep, jump and suspension. The amount of sediment is defined as the amount of sand carried by unit area or unit width per unit time. Since the amount of sediment is mainly affected by the wind velocity, the sand mass and the underlying surface characteristics, the sand will be deposited at the corresponding position when the velocity of the moving sand is reduced to its starting wind velocity caused by those factors.

Wind tunnel test: The wind tunnel structure commonly includes experimental section, voltage regulating seam, expansion section, corner deflector, power driven system, stability section, rectifier, shrinkage and measurement control system. The reliability of the wind tunnel simulation experiment depends on the similarity between the experimental conditions and the actual situation in the field. It is necessary to satisfy the geometric similarity, movement similarity and dynamic similarity, and because the steady flow of viscous incompressible fluid has the self-moldability and stability, that is, under certain conditions, the model's flow field has a similar distribution to the prototype flow field, which makes the wind tunnel test authentic.

Numerical simulation: The simulation is based on the wind tunnel test, that is, the experimental process cannot be carried out by numerical simulation based on the achievable wind tunnel results. Firstly, the solid model needs to be established, and the computational fluid dynamics (CFD) software is used to partition the mesh and simulate under the premise of reasonably setting the corresponding calculation and control parameters, and check and analyse the results.

The results of theoretical analysis can reveal the flow law of fluid, which can reflect the real changes of the actual model, and has universal applicability. The model of RANS equation's theory is based on the theoretical knowledge of the turbulence, experimental data or direct numerical simulation results, Reynolds stress to make various assumptions, making assumptions about the Reynolds stress, which assumes a variety of empirical and semi empirical constitutive relations, so that the average Reynolds equation of turbulence can be figured out. The fluid simulation process should satisfy the continuous equation, the momentum equation, the k equation and the μ equation, as follows:

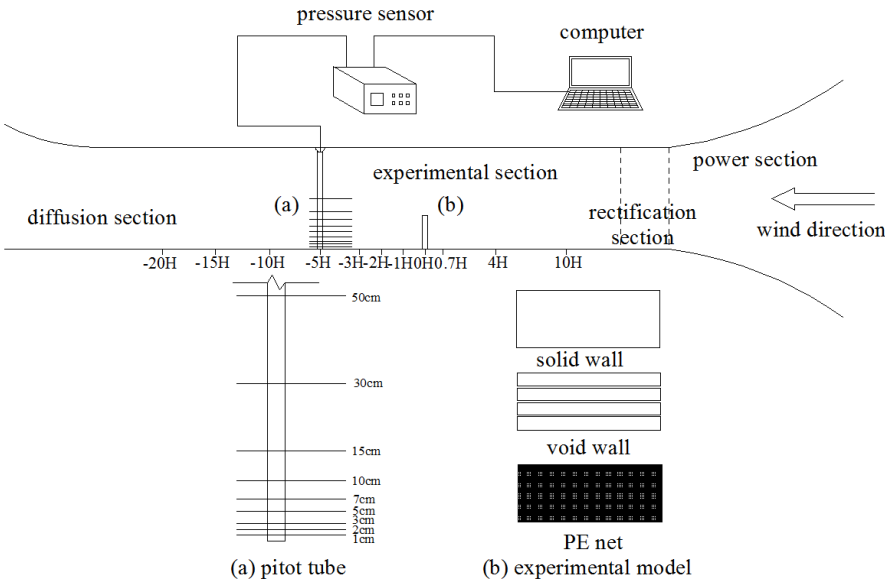

Fig. 2: The layout of wind tunnel experiment.

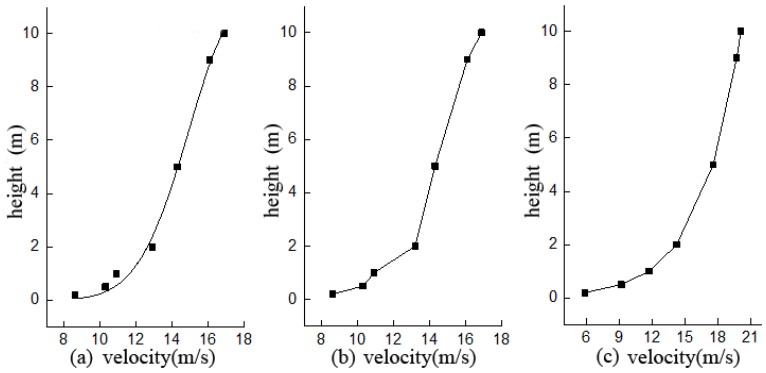

Fig. 3: Wind velocity fitting values (a), measured values (b) and theoretical calculated values (c) at different heights.

$$\frac{\partial \rho}{\partial t} + \nabla \bullet (\rho U) = 0 \quad ...(1)$$

$$\frac{\partial (\rho \gamma_i)}{\partial t} + \nabla \bullet (\rho \gamma_i \nabla \vec{v}) = \rho \bullet (\frac{\partial \gamma_i}{\partial t} + \vec{v} \bullet grad\, \gamma_i) \quad ...(2)$$

$$\frac{\partial (\rho k)}{\partial t} + \nabla \bullet (\rho U k) = \nabla \bullet [(\mu + \frac{\mu_t}{\sigma_k}) \nabla k] + P_k - \rho \varepsilon \quad ...(3)$$

$$\frac{\partial (\rho \varepsilon)}{\partial t} + \nabla \bullet (\rho U \varepsilon) = \nabla \bullet [(\mu + \frac{\mu_t}{\sigma_{\varepsilon RNG}}) \nabla \varepsilon] + \frac{\varepsilon}{k} (C_{\varepsilon_{1RNG}} P_k - C_{\varepsilon_{2RNG}} \rho \varepsilon) \quad ...(4)$$

WIND TUNNEL TEST

Wind tunnel experiments were carried out in the Chinese Academy of Sciences Cold and Arid Regions Environmental and Engineering Research Institute. The wind tunnel has a length of 38m, a test section length of 21m, and the wind tunnel cross section of 1.2m × 1.2m. The wind tunnel is a DC blown wind tunnel, which is composed of dynamic section, rectification section, sand supply device, test section and diffusion section. The wind tunnel experimental model layout is shown in Fig. 2, and the model height is 10cm.

The profile wind velocity will be adopted in the simulation calculation due to the high turbulence caused by the friction of the underlying surface and the effect of thermalization when the airflow is moving in the near-surface layer. In the neutral stratification atmosphere, the wind velocity is mainly affected by the surface friction, and the wind velocity changes in logarithmic form along the height direction as the friction decreases with increasing of height, which is called Prandtl von Karman logarithmic velocity distribution law, shown as below:

$$u_x = \frac{u_*}{k} \ln \frac{z}{z_0} \quad ...(5)$$

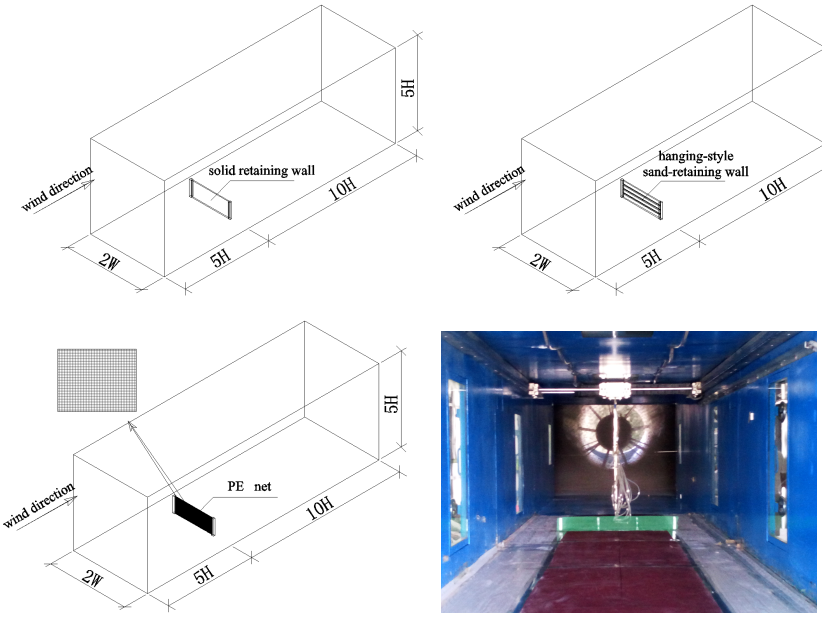

Fig. 4: Three numerical calculation models and wind tunnel experimental model

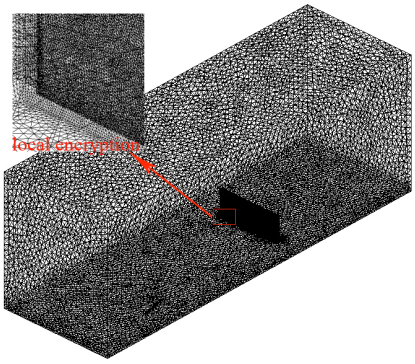

Fig. 5: PE net meshing results.

In the formula, u_* stands for the friction velocity, $u_* = \frac{\sqrt{\tau}}{\rho}$; u_x represents the wind velocity at height of Z whose unit is m/s; Z_0 represents the surface roughness coefficient, that is, the height whose unit is m/s where the wind velocity is zero; k represents the Carmen coefficient whose general value is 0.4. In this paper, after a certain proportion of adjustment, it drew the relationship curves (Xin et al. 2016) of wind velocity fitting values, measured values and theoretical calculated values at different heights through the field observation and wind tunnel simulation experiment and the fitting software called Origin, where the different height wind velocity fitting values are encoded by UDF as the inlet profile wind velocity in numerical simulation, as shown in Fig. 3.

NUMERICAL SIMULATION

Pre-processing

Model establishment: The study selected the universal application of the solid retaining wall, the void wall and PE net for simulation calculation, and analysed its benefits in sand-blocking. The model was selected according to the actual engineering size, that is, choosing the solid retaining wall whose height is 1600mm and thickness 100mm, the hanging-style sand-retaining wall with 30% porosity which was widely used, and PE net with 55% porosity specified as JZSPE1600Lu32. Under the condition of not affecting the actual effect of the sand-proof structures, the size of the calculation domain was defined as follows: 15H length, 8000mm width and 5H height (H is the wall height). The corresponding model established by CAD is shown in Fig. 4.

Mesh generation: The PE net model has the characteristics of a small pore and slender wire diameter, which is not conducive to grid division, so it was set to a porous area when simulating it. At this point, the grid was divided by a tetrahedral mesh method that is simple and conducive to initialize as the three models are relatively simple. In order to improve the accuracy of subsequent calculations while ensuring convergence with the computing domain grid, the grid size was unified as 200mm with the local region encrypted, that is, the structure of the wind side and the leeward side of the grid size of 20mm using the automatic grid division method. The meshing results of the PE net are shown in Fig. 5, and the grid

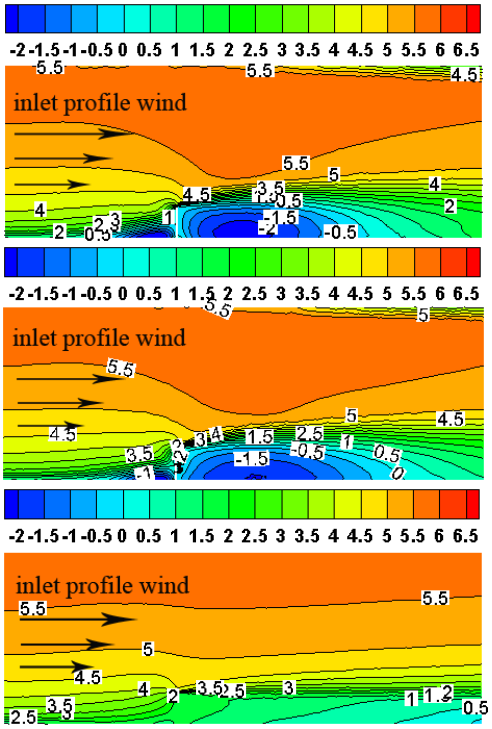

Fig. 6: The velocity nephogram in the centre normal plane of three models at the velocity of 6m/s.

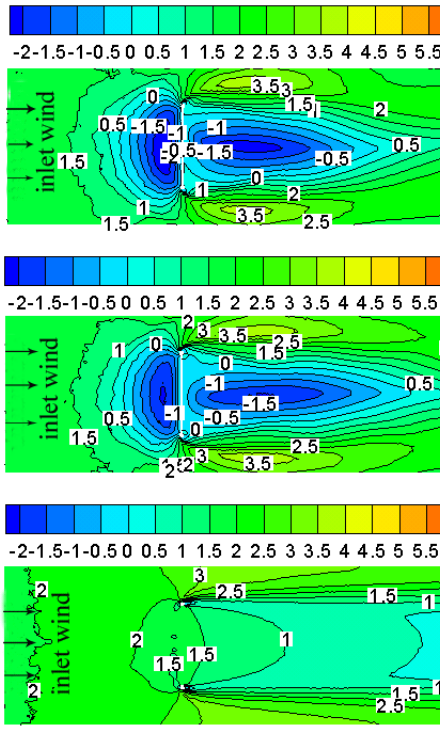

Fig. 7: The velocity nephogram of three models in the position of Z = 20cm at the velocity of 6m/s.

information includes 110250 nodes, 1255720 mesh faces and 621512 grid cells with a grid quality of 0.2.

Simulation Calculation

Boundary condition setting: According to the principle of aerodynamics, the airflow was defined as an incompressible flow when the Mach number is less than 0.3 (Cheng et al. 2013), so the inlet condition of calculation model was set as velocity-inlet because the Mach number of the wind-blown-sand-two phase flow is less than 0.3, and according to the relationship between sand incipience and wind velocity, in the simulation, four kinds of inlet wind velocities were set, which are wind velocity profiles with 6m/s, 9m/s, 12m/s and 15m/s as the centre wind velocity respectively. The left and right sides were set as symmetrical boundary conditions, and the outlet of the computational domain was set as pressure-outlet, the upper boundary condition was also set as the pressure-outlet taking the influence of the atmospheric boundary layer into account.

Calculation parameter settings: It was necessary to set the calculation parameters after selecting the standard two-equation model in the simulation calculation, such as air density defined as 1.225kg·m^{-3}, viscosity defined as 1.789×10^{-5}Pa·s; and setting the viscosity resistance coefficient and the internal resistance coefficient as 1.7×10^{8} and 1300 respectively, in the process of PE net simulation with porous media conditions, but the difference between the mainstream direction and the non-mainstream direction value was not allowed more than 1000 times. Monitoring convergence accuracy should be less than 10^{-3} using the default value to the calculation method and control condition.

RESULTS AND DISCUSSION

Post-processing: We used the hydrodynamic post-processing module named CFD-Post and TECPLOT to obtain the velocity cloud picture of the three wind-resisting structures by setting the relevant parameters, as shown in Fig. 6.

It could be seen that there was the vortex region in the front of or behind the solid wall under the condition of the inlet profile velocity whose centre velocity was 6m/s , and forming an extrusion uptrend area over the top of the wall, and the main reason was that the solid wall was a blunt body with a pointed edge. When the airflow passed, it was squeezed at the top of the retaining wall to create a separation and forming a strong shear layer (Pang et al. 2011). The main vortex zone was formed in the 2H front of the retaining wall and distributed in the lower half of the height of the retaining wall and affected the change of wind velocity in the range of about 4H length in the front of the barrier. The airflow, which passed through the upper half of the retain-

Table 2: The extreme velocity values in the centre normal plane of three models at different wind velocities.

Inlet velocity	Solid wall		Hanging-style plate wall		PE net	
	Minimum	Maximum	Minimum	Maximum	Minimum	Maximum
6m/s	-2.707	5.929	-2.470	5.929	-0.051	5.877
9m/s	-4.045	8.815	-3.689	8.848	-0.606	8.758
12m/s	-5.414	11.800	-4.949	11.780	-0.638	11.700
15m/s	-6.794	14.730	-6.222	14.770	-0.737	14.050

ing wall, was influenced by the retaining of the wall and the free atmospheric pressure at the top of the wall so that it flowed over the solid wall at a greater velocity and followed by the formation of the uptrend area, which in turn affected the wind velocity changes behind the retaining wall. Behind the wall about 5H length of the retaining wall and a large reflux area was formed, which was distributed in the whole height of the retaining wall and affected the wind velocity value in the range of about 20H behind the wall, that is, the wind velocity changed obviously under the influence of the retaining wall. In the same scale size, the effect of the hanging plate with 30% porosity on wind velocity was weaker than that of the solid wall, but vortex zone also formed in front of or behind the wall, and forming an extrusion uptrend area in the top of the plate at the same time; and the vortex area with the smaller range was formed in front of the plate, which mainly distributed in the range of the one-third height of the plate from the ground and 1.5H length in the horizontal direction, and the wind velocity of the vortex zone was smaller than that of the solid retaining wall, and the influence range was weakened. The hanging plate retaining wall only had porosity of 30%, when the inlet wind flowed through the hanging plate, most of the airflow would squeeze up and form the increased velocity region on the top of the hanging plate and affect the subsequent wind velocity changes due to the blocking effect of the plate. And the airflow through the void weakened the strength of the re-flow zone behind the barrier, and the core vortex area was not obvious, but the influence range increased with the impact of the incoming flow, that is, the wind velocity change under the effect of the plate was obvious.

The influence of the PE net with 55% porosity on wind velocity was true and reliable, which was simulated by the porous medium condition. No obvious eddy current was formed in the whole calculation domain (small vortex was formed at larger wind velocity), the impact in the front of the net on the inlet wind velocity was not obvious, and there was only a small change in the location where the net set. It formed a clear rectification area behind the net, that is, the entrance profile wind was weakened and rectified to almost the same wind velocity under the influence of the uniform hole of the net, and there was no erosion on the surface and column because of the no emergence of eddy current, which was not only conducive to the deposition of sand, but also played a good sand control effect.

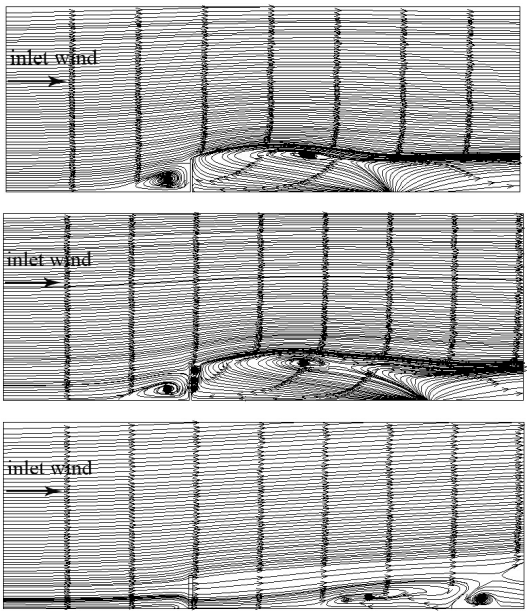

Fig. 8: The streamlines in the centre normal plane of three models at the velocity of 15m/s.

It could be seen that the vortex area in the front of or behind the solid wall was distributed in the whole length of the retaining wall, and the velocity of the core vortex zone was larger, which was easy to produce wind erosion phenomenon (Fig. 7). When the flow gone through the solid retaining wall, there would also be acceleration vortex zone formed at both sides of the wall because of the reserved space in the computational domain, and the acceleration zones formed on both sides of the retaining wall were symmetrically distributed due to the reasonable setting of the simulation parameters. The negative pressure zone behind the retaining wall was distributed within 6H in the horizontal direction and one third of the middle of the retaining wall length. The effect of the hanging plate retaining wall on the incoming flow was similar to that of the solid retaining wall in the whole calculation domain, the difference was that the core reflux area in the front of the board was smaller, and the vor-

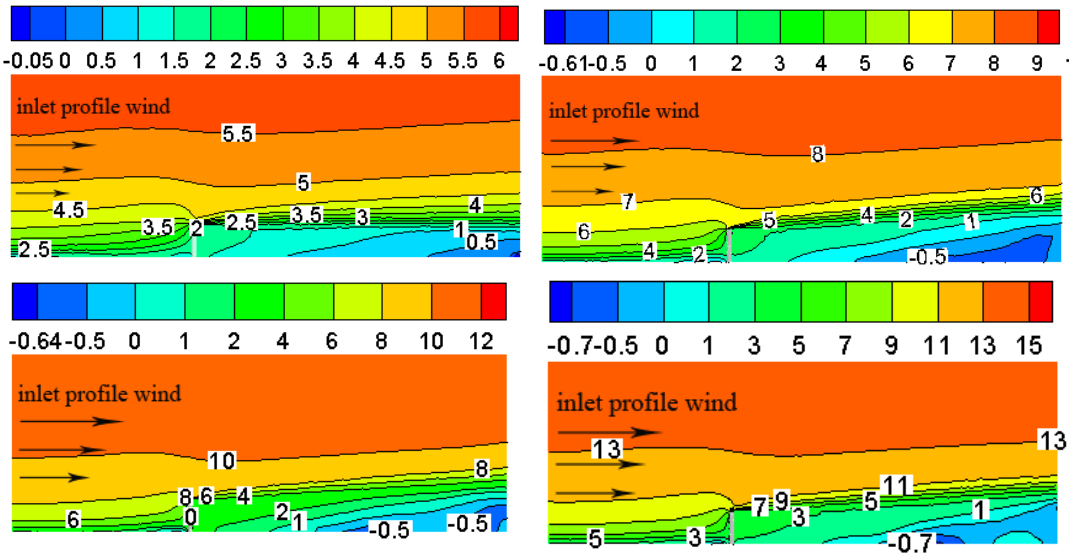

Fig. 9: The velocity nephogram in the centre normal plane of PE net at different wind velocities.

tex behind the barrier was distributed in the 7.5H longitudinal length range, which increased the distance by 1.5H compared to the physical retaining wall. There was no vortex zone behind the PE net in the condition of the inlet profile wind velocity whose central velocity was 6m/s, and the velocity change is more uniform behind the net, which had the same effect in the actual engineering.

Fig. 8 showed the vector streamlines of the flow field around the three models under the profile wind velocity whose centre velocity was 15m/s, which was added manually through the post-processing software TECPLOT, and the local eddy or complicated streamline would be added densely. The extreme values of the velocity in that section at different wind velocities are provided in Table 2.

It could be seen that the trend of the flow field around the PE net under the four kinds of wind velocity was similar, there was no obvious eddy current area, but the stable and little change flow field distribution behind the net. With the increase of wind velocity, the velocity streamline changes at the top of the PE net was more obvious and showed a rising trend, that is, the angle between the streamline beyond the PE net and the horizontal direction gradually increased and reached to a steady state (Fig. 9). The increasing wind velocity would lead to a certain range of zero velocity zone appeared in certain positions (about 3.5H) behind the net, but rarely vortex. And at the bottom of the net, there would be a small range of deceleration zones with the increase of the wind velocity, only reflected in the larger wind velocity ($V > 12\text{m}/\text{s}$). In general, the flow field tended to be stable under the influence of the PE net, and the velocity was greatly weakened and easy to reduce to the starting wind velocity of the sand through the rectification of the net, which was conducive to the deposition of sand particles and played a good sand-blocking effect without wind erosion hazards to the surface.

Wind velocity profile change: The wind velocity profile under the open field, also called barrier-free model, was fitted through the wind tunnel test and the theoretical analysis, and it exhibited a changing trend like exponential function due to the ground frictional resistance (Fig. 10). The wind velocity profile was imported into the hydrodynamic software as an inlet velocity condition for simulation calculations by UDF programming. It could be seen that the wind velocity profile at different locations had similarity in the vertical direction and there was a certain law in the range of 2H behind the barrier. Under the profile wind velocity whose centre wind velocity was 6m/s condition, the influence of the solid wall on the wind velocity has shown in the deep red curve, and there was a swirl zone at 0.2H behind the barrier. And the velocity firstly reduced to -0.6m/s along the height of the solid wall, which was located in the height of the wall at 0.5H. And then, the velocity suddenly changed to 3.2m/s after increasing to 0m/s, which was located in the top of the wall and it is caused by a sudden change of pressure. But there was the growth zone above the height of the wall because of the existence of the retaining wall, which is the case where the velocity above the retaining wall was greater than the velocity of the empty field. The velocity curve under the influence of the hanging-style sand-retaining wall was described by a blue curve, there was no obvious eddy current area behind the barrier at the position of 0.2H. Some of the incoming streams were directly poured into the

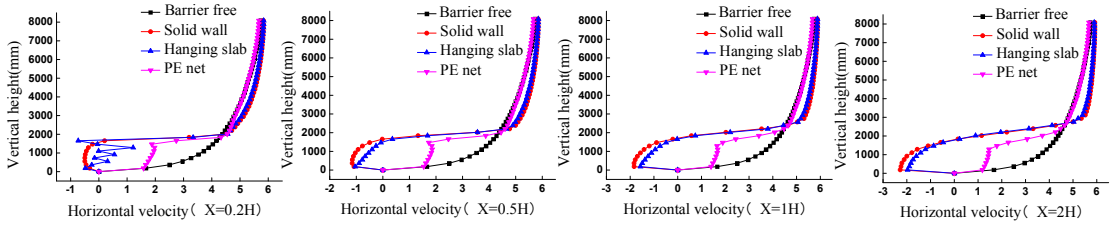

The wind velocity profile in the center normal plane different positions behind the barrier at the velocity of 6m/s

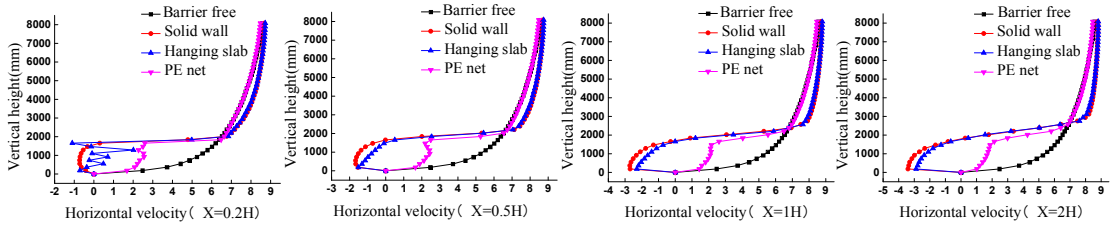

The wind velocity profile in the center normal plane different positions behind the barrier at the velocity of 9m/s

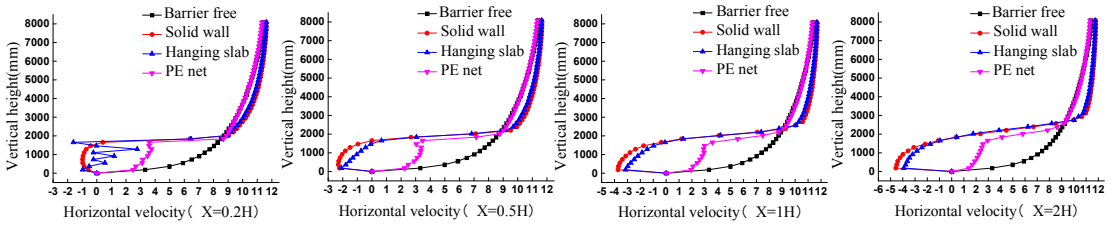

The wind velocity profile in the center normal plane different positions behind the barrier at the velocity of 12m/s

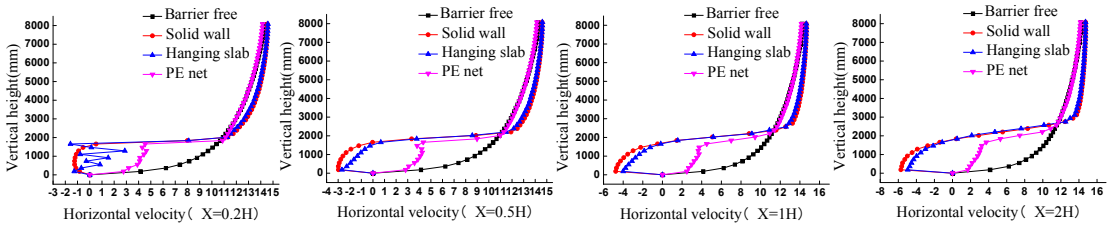

The wind velocity profile in the center normal plane different positions behind the barrier at the velocity of 15m/s

Fig. 10: The wind velocity profile in the centre normal plane different positions behind three models at different wind velocities.

hole from the hole, resulting in positive and negative velocities alternating in the corresponding position, and the wind velocity changed suddenly due to the rapid change of airflow on top of the hanging plate, that is, from -0.8m /s to 3.4m/s, and forming the growth zone. And the growth area on the top of the hanging plate was weakened contrasted to the solid wall due to the part of the hole. The PE net impact on the wind velocity curve was shown by the light red curve, there was no eddy current area, the velocity change in the height range of the net was small, concentrated between 1.6m/s and 1.9m/s, and the velocity variation above the net was similar to that of the barrier-free model.

The effect of the solid wall and the PE net on the velocity at X = 0.5H was the same as at the X = 0.2H position. The change of the airflow was more stable under the influence of the hanging-style, sand-retaining wall. And the influence of airflow from the plate hole did not exceed 0.5H, and the kinetic energy carried by the airflow gradually spread behind the barrier. The eddy current intensity along the height direction was smaller than that influenced by the solid wall at the corresponding position of X = 0.5H, that is, the velocity was firstly reduced to -1.1m/s and then gradually increased to 0m/s and then mutated to a similar trend to that in the case of the barrier-free model.

It could be seen that with the increase of the distance behind the barrier, the minimum value of the wind velocity

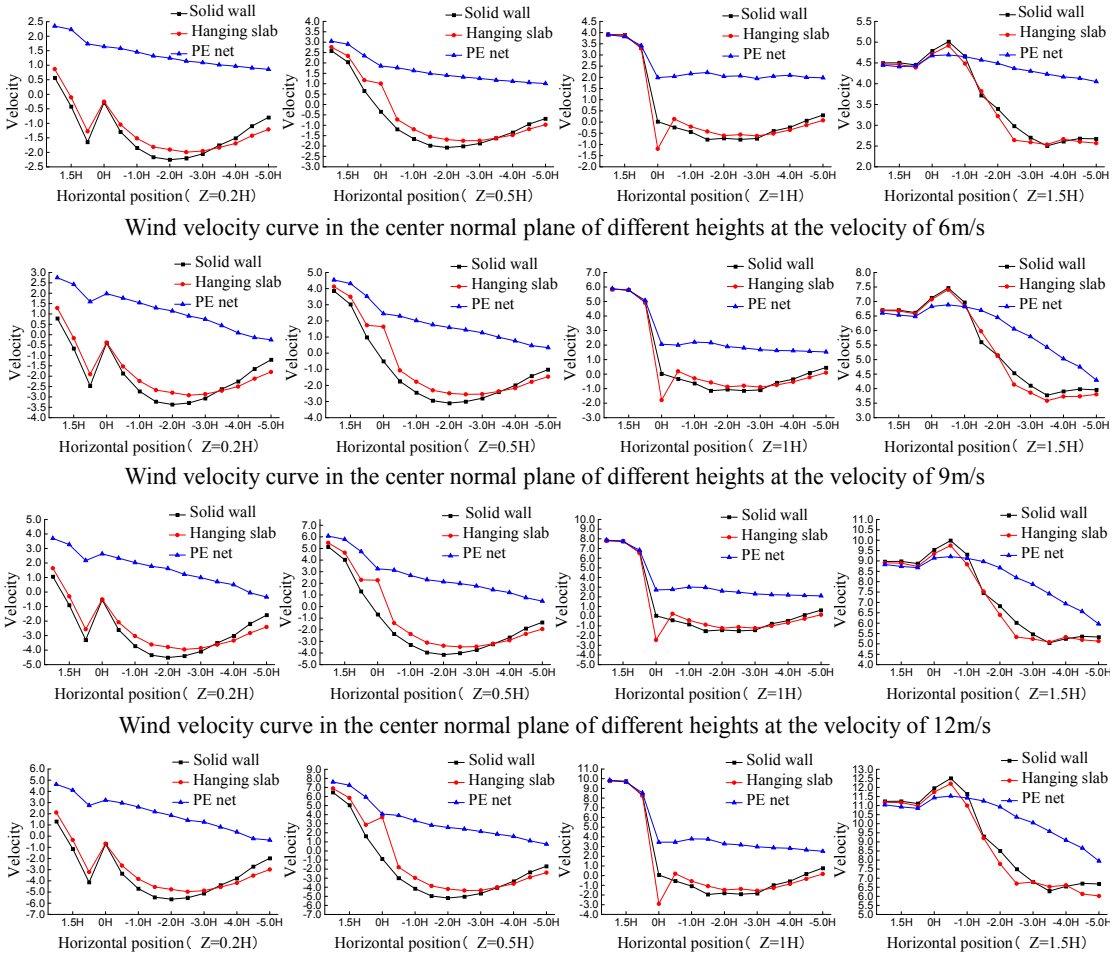

Fig. 11: Three models wind velocity curve in the centre normal plane of different heights at different wind velocities.

under the influence of the retaining wall was gradually increasing, that is, the intensity of the vortex zone was gradually increasing and the velocity increase amplitude of the growth zone was also gradually increasing. The velocity change under the influence of the hang-style, sand-retaining wall was more complex at the position of X=0.2H. With the position of the back, the intensity of the eddy current zone showed an increasing trend. And the change of the velocity in growth zone was similar to that of the solid retaining wall, but the velocity value was smaller in corresponding position. The velocity profile change was more stable under the influence of the PE net. With the increase of wind velocity, the effect of the three obstacles on the wind velocity profile was similar at different locations. The difference is that the velocity value would increase relative to the corresponding position with the increase of the inlet wind velocity, such as, behind the barrier at the position of 0.2H and under the influence of the solid wall, the vortex velocity was decreasing with the increase of the entrance wind velocity, that is, eddy current strength was increasing.

Velocity change in special position: It selected the velocity value of the centre normal direction along the height direction in Z=0.2H, Z=0.5H, Z=1H, Z=1.5H, and analysed the effect of three models on wind velocity (Fig. 11). The velocity change behind the barrier was relatively stable in the four locations under the influence of the wind velocity of 6m/s, and the velocity in the front of the net was greater than the velocity after the net in the high range of the net. The velocity began to decrease with the increase of the distance behind the net and tended to be stable after a transient increase at the location of the net where it was set at the height of Z=1.5H, which indicated that the existence of the network had a certain obstruction to the flow and there would be a small range of growth zones at the top of the net.

The eddy current in the front of the barrier mainly distributed below half the height of the retaining wall and the vortex behind the barrier distributed throughout the height of the retaining wall under the influence of the solid retaining wall, and the squeeze uptrend area distributed within 1H behind the barrier. With the increase of wind velocity, the change trend of the influence of different models on velocity was kept constant, and the velocity value at the corresponding horizontal position was increased.

CONCLUSIONS

1. The wind tunnel experiment can accurately measure the wind velocity change at different positions along the normal direction of the sand barrier by the heat sensitive anemometer under the control of reasonable similarity condition, which can reflect the influence of the actual engineering barriers on the profile flow, which has great reference value.
2. It can comprehensively and systematically reflect the real situation of the various sand-blocking structures in the field environment through the simulation by the fluid dynamics software. The analysis shows that the solid sand-retaining wall and hanging-style, sand-retaining wall with 30% porosity will form the swirl zone behind the barrier and the growth zone at the top of the wall under the different wind velocities, which is not conducive to the deposition of sand, and the sand whose velocity is weakened, which is influenced by the eddy current, will erode the surface and foundation and reduce the life of sand barrier finally. But in smaller wind velocity areas, a range of gravels can be laid behind the two barriers to weaken the effects of eddy currents.
3. It is found that the PE net with 55% porosity can not only reduce the flow velocity and form a large scale (0~15H) stable deceleration zone behind the net, but also almost no eddy current appear behind the barrier, which has a high sand-controlling benefits. PE net is made of environmentally friendly resin fibre which has excellent anti-aging properties and anti-wind erosion ability, and net-type sand barrier is flexible to combine, easy to install, and it can meet the sand-blocking and sand fixation needs in different environments with broad application prospects.

ACKNOWLEDGMENTS

This research is supported by the National Natural Sciences Foundation of China (51568057, 51268050, 50908152) and the Natural Sciences Foundation of Shihezi University (2014ZRKXJQ06). The authors also thank the anonymous reviewers and editor who helped to improve the quality of this paper.

REFERENCES

Bagnold, R.A. 1941. The Physics of Blown Sand and Desert Dunes. London, Methuen.

Cheng, J.J., Lei, J.Q., Li, SH.Y. and Wang, H.F. 2016a. Effect of hanging-type sand fence on characteristics of wind-sand flow fields. Wind and Structures, 22(5): 555-571.

Cheng, J.J., Lei, J.Q., Li, SH.Y., Wang, H.F. 2016b. Disturbance of the inclined inserting-type sand fence to wind-sand flow fields and its sand control characteristics. Aeolian Research, 21: 139-150.

Cheng, J.J. and Pang, Q.D. 2013. Study on the aerodynamic characteristics of the vehicles under the wind-retaining structure of the Gobi strong wind area. Railway Standard Design, 01: 01-04.

Ding, G.D. 2010. Wind and S and Physics (2nd Edition). Beijing: China Forestry Publishing House, pp. 65.

Gao, G.J., Tian, H.Q., Yao, S., Liu, T.H. and Bi, G.H. 2004. Effects of strong cross wind along Lanzhou-Xinjiang railway on the overturning stability of vehicles. Journal of the China Railway Society, 26(4): 36-40.

He, P. 2013. Design of railway protection engineering in blown sand area. Railway Construction, 5: 112-115.

Hu, P.X. 2003. A brief talk on present situation of sandy land and countermeasures in China. Forestry Science, 5: 140-146.

Kang, X.G., Li, S.H.Y., Ma, X.X., Wang, H.F., Lei, J.Q. and Wang, S.H.J. 2015. Comparison and analysis of sediment concentration of different combination spacing of two sand blocking nylon net. Arid Research, 2: 347-353.

Kang, X.G., Li, S.H.Y., Wang, H.F., Ma, X.X. and Lei, J.Q. 2015. Comparison of sediment morphology characteristics of and blocking nylon net with different combination space. Arid Area Geography, 2: 283-291.

Li, X.J. and Jiang, F.Q. 2016. Analysis of response law of blown sand flow to wind-retaining wall in Gobi area. Railway Standard Design, 3: 47-51+60.

Pang, Q.D., Liu, J.J., Cheng, J.J. and Jiang, F.Q. 2011. Study on vorticity length and sediment in windward wall of Gobi railway. Journal of Shihezi University (Natural Science Edition), 29(5): 629-632.

Ren, Z.S., Xu, Y.G., Wang, L.L. and Qiu, Y.Z.H. 2006. Study on the influence of strong crosswind on high velocity train operation safety. Journal of the China Railway Society, 28(6): 46-50.

Sun, Q.J., Wang, T., Han, Z.H.W. and Zhang, W.M. 2004. Study on blown sand hazard along northern Xinjiang railway. China Desert, 3: 182-186.

Xin, G.W., Cheng, J.J., Jing, W.H., Zhang, F., Wang, L. and Zhi, L.Y. 2016. Numerical simulation of flow profile's influence on blown sand flow and sand accumulation-take the sand-retaining wall as an example. Journal of Arid Land Research, 03: 672-679.

Yang, M.Z.H., Yuan, X.X., Lu, Z.H.J. and Huang, H.J. 2008. Wind tunnel experimental study on aerodynamic performance of Qinghai-Tibet railway trains under strong crosswind. Experimental Fluid Mechanics, 22(1).